Some computational results for generalized pressure Schur complement eigenvalues of the surface Stokes problem

Alexander Zhiliakov*

February 20, 2019

1 Bilinear forms and matrices

We set $n_{\mathbf{A}}$ to be the number of velocity d.o.f. and $n_{\mathbf{S}}$ to be the number of pressure d.o.f. Vector stiffness, divergence, pressure mass, normal stabilization, and full stabilization matrices resulting from Trace FEM discretization of the surface Stokes problem [1] are defined via

$$\begin{aligned}
\langle \mathbf{A}\,\bar{\mathbf{u}}, \bar{\mathbf{v}}\rangle &= \int_\Gamma \big(E_s(\mathbf{u}) : E_s(\mathbf{v}) + \mathbf{u}\cdot\mathbf{v} + \tau\, u_N\, v_N\big)\,\mathrm{d}s + \rho_u \int_{\Omega_h^\Gamma} ([\nabla\mathbf{u}]\,\hat{\mathbf{n}})\cdot([\nabla\mathbf{v}]\,\hat{\mathbf{n}})\,\mathrm{d}\mathbf{x}, \quad \mathbf{A}\in\mathbb{R}^{n_{\mathbf{A}}\times n_{\mathbf{A}}},\\
\langle \mathbf{B}\,\bar{\mathbf{u}}, \bar{\mathbf{q}}\rangle &= -\int_\Gamma q\,\mathrm{div}_\Gamma\,\mathbf{u}\,\mathrm{d}s, \quad \mathbf{B}\in\mathbb{R}^{n_{\mathbf{S}}\times n_{\mathbf{A}}},\\
\langle \mathbf{M}_0\,\bar{\mathbf{p}}, \bar{\mathbf{q}}\rangle &= \int_\Gamma p\,q\,\mathrm{d}s, \quad \mathbf{M}_0\in\mathbb{R}^{n_{\mathbf{S}}\times n_{\mathbf{S}}},\\
\langle \mathbf{C}_n\,\bar{\mathbf{p}}, \bar{\mathbf{q}}\rangle &= \rho_p \int_{\Omega_h^\Gamma} \frac{\partial p}{\partial\hat{\mathbf{n}}}\frac{\partial q}{\partial\hat{\mathbf{n}}}\,\mathrm{d}\mathbf{x}, \quad \mathbf{C}_n\in\mathbb{R}^{n_{\mathbf{S}}\times n_{\mathbf{S}}},\\
\langle \mathbf{C}_{\text{full}}\,\bar{\mathbf{p}}, \bar{\mathbf{q}}\rangle &= \rho_p \int_{\Omega_h^\Gamma} \nabla p\cdot\nabla q\,\mathrm{d}\mathbf{x}, \quad \mathbf{C}_{\text{full}}\in\mathbb{R}^{n_{\mathbf{S}}\times n_{\mathbf{S}}},
\end{aligned} \tag{1}$$

respectively. We use notations as in [1], in particular, Ω^h_Γ is the domain consisting of tetrahedra cut by Γ. Here $\bar{\mathbf{u}}$ denotes a vector of d.o.f. corresponding to a FE interpolant $\mathbf{u}$ (analogously for $\bar{\mathbf{p}}$ and p). Mesh-dependent parameters are set as

$$\tau = h^{-2}, \quad \rho_u = \rho_p = h, \tag{2}$$

and h is the typical mesh size for tetrahedra from Ω_h^Γ. Γ is chosen either as the unit sphere or torus, $\Gamma = \Gamma_{\text{sph}}$ or $\Gamma = \Gamma_{\text{tor}}$ (see Figure 1).

We also define matrices

$$\begin{aligned}
\mathbf{C}_0 &\coloneqq \mathbf{0},\\
\mathbf{M}_n &\coloneqq \mathbf{M}_0 + \mathbf{C}_n,\\
\mathbf{M}_{\text{full}} &\coloneqq \mathbf{M}_0 + \mathbf{C}_{\text{full}}.
\end{aligned} \tag{3}$$

*Department of Mathematics, University of Houston, Houston, Texas 77204 (alex@math.uh.edu).

We are interested in (generalized) extreme eigenvalues of the pressure Schur complement matrices

$$\begin{aligned} \mathbf{S}_0 &\coloneqq \mathbf{B}\,\mathbf{A}^{-1}\,\mathbf{B}^T, \\ \mathbf{S}_n &\coloneqq \mathbf{S}_0 + \mathbf{C}_n, \\ \mathbf{S}_{\text{full}} &\coloneqq \mathbf{S}_0 + \mathbf{C}_{\text{full}}, \end{aligned} \tag{4}$$

i.e. in solving

$$\mathbf{S}_\star\,\mathbf{x} = \lambda\,\mathbf{M}_\star\,\mathbf{x}, \tag{5}$$

where "$\star$" stands for "0," "n," or "full." We denote by $0 = \lambda_1 < \lambda_2 \le \cdots \le \lambda_{n_\mathbf{S}} = O(1)$ the spectrum of (5).

2 Solution description

Computing $\mathbf{A}^{-1}$ in (4) becomes troublesome already for $h = 5.21 \times 10^{-2}$ ($n_\mathbf{A} = 32736$ for $\mathbf{u} \in \mathbf{P}_1$ FE space): although $\mathbf{A}$ is sparse, $\mathbf{A}^{-1}$ is dense and consumes 8.5+ GB in double-precision arithmetic. A quick research showed that `Mathematica` has no built-in matrix-free eigenvalue routines. `Intel MKL`'s FEAST algorithm for computing (generalized) eigenvalues in an interval is suitable for matrix-free implementations; however, it requires some expensive operations to be implemented (e.g. matrix-matrix multiplications $\mathbf{Y} \leftarrow \mathbf{S}_\star\,\mathbf{X}$, $\mathbf{Y} \leftarrow \mathbf{M}_\star\,\mathbf{X}$ and approximating the action of inverses in the form $\mathbf{y} \leftarrow (\sigma\,\mathbf{M}_\star - \mathbf{S}_\star)^{-1}\,\mathbf{x}$).

Taking this into account, instead of (5) we consider a perturbed[1] problem

$$\underbrace{\begin{bmatrix} \mathbf{A} & \mathbf{B}^T \\ \mathbf{B} & -\mathbf{C}_\star \end{bmatrix}}_{\mathcal{A}_\star \coloneqq} \begin{bmatrix} \mathbf{x} \\ \mathbf{y} \end{bmatrix} = \mu \underbrace{\begin{bmatrix} \epsilon\,\mathbf{A} & \\ & \mathbf{M}_\star \end{bmatrix}}_{\mathcal{M}_\star^\epsilon \coloneqq} \begin{bmatrix} \mathbf{x} \\ \mathbf{y} \end{bmatrix} \tag{6}$$

with $0 < \epsilon \ll 1$. For $\mathcal{A}_0$ and $\mathcal{M}_0^\epsilon$ we have

$$\mu = -\lambda + o(1) \quad \text{or} \quad \epsilon^{-1} + \lambda + o(1), \qquad \epsilon \to 0. \tag{7}$$

This makes it easy to pick only "correct" eigenvalues. To ease the computation further we replace the $(1,1)$-block of $\mathcal{M}_\star^\epsilon$ with $\epsilon\,\mathbf{I}$.

To make sure that results are consistent we solve (6) for $\epsilon = 10^{-5}$ and $\epsilon = 10^{-6}$; for the coarse mesh levels we also check that the direct solution of (5) and the iterative one for (6) coincide.

3 Numerical results: dependency of the spectrum on the mesh size

[1]The majority of generalized eigenvalue solvers require left-hand-side matrix to be Hermitian and right-hand-side matrix to be Hermitian **positive definite**; that's why we need to introduce $\epsilon > 0$.

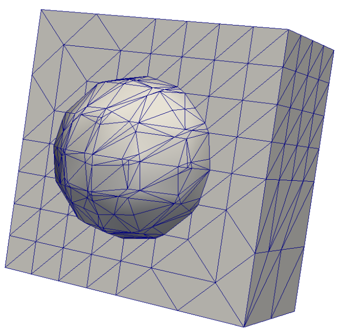

(a) $h = 8.33 \times 10^{-1}$

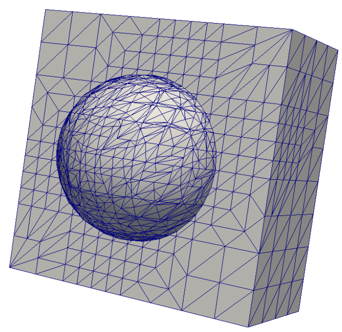

(b) $h = 4.17 \times 10^{-1}$

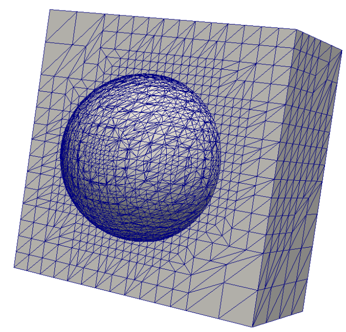

(c) $h = 2.08 \times 10^{-1}$

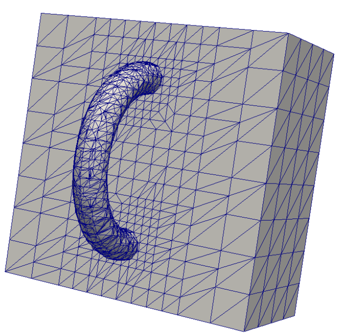

(d) $h = 2.08 \times 10^{-1}$

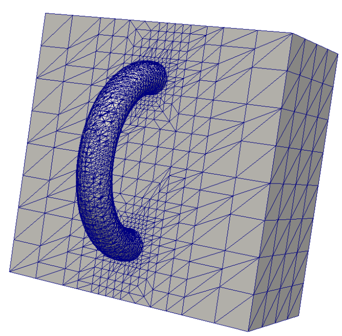

(e) $h = 1.04 \times 10^{-1}$

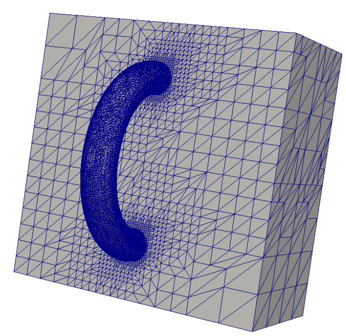

(f) $h = 5.21 \times 10^{-2}$

Figure 1: First three mesh levels for Γ_{sph} (top) and Γ_{tor} (bottom)

Table 1: Spectrum of (5) for $\mathbf{P}_1 - P_1$

(a) $\Gamma = \Gamma_{\text{sph}}$

h	$n_{\mathbf{A}}$	$n_{\mathbf{S}}$	$\mathbf{S}_0$		$\mathbf{S}_n$		$\mathbf{S}_{\text{full}}$	
			λ_2	$\lambda_{n_\mathbf{S}}$	λ_2	$\lambda_{n_\mathbf{S}}$	λ_2	$\lambda_{n_\mathbf{S}}$
8.33×10^{-1}	153	51	1.32×10^{-2}	1.42	7.48×10^{-1}	1.13	9.58×10^{-1}	1.06
4.17×10^{-1}	570	190	5.12×10^{-3}	1.04	5.77×10^{-1}	1.	8.54×10^{-1}	1.
2.08×10^{-1}	1992	664	4.4×10^{-3}	7.93×10^{-1}	3.87×10^{-1}	1.	6.71×10^{-1}	1.
1.04×10^{-1}	8292	2764	2.01×10^{-3}	7.79×10^{-1}	2.19×10^{-1}	1.	5.82×10^{-1}	1.
5.21×10^{-2}	32736	10912	6.04×10^{-5}	9.81×10^{-1}	1.17×10^{-1}	1.	5.37×10^{-1}	1.
2.6×10^{-2}	131592	43864	3.53×10^{-5}	8.67×10^{-1}	5.72×10^{-2}	1.	5.16×10^{-1}	1.
1.3×10^{-2}	525864	175288	2.16×10^{-6}	7.34×10^{-1}	2.84×10^{-2}	1.	5.04×10^{-1}	1.

(b) $\Gamma = \Gamma_{\text{tor}}$

h	$n_{\mathbf{A}}$	$n_{\mathbf{S}}$	$\mathbf{S}_0$		$\mathbf{S}_n$		$\mathbf{S}_{\text{full}}$	
			λ_2	$\lambda_{n_\mathbf{S}}$	λ_2	$\lambda_{n_\mathbf{S}}$	λ_2	$\lambda_{n_\mathbf{S}}$
2.08×10^{-1}	972	324	5.04×10^{-2}	4.93	2.84×10^{-1}	1.35	3.64×10^{-1}	1.19
1.04×10^{-1}	4740	1580	2.99×10^{-3}	3.83	1.58×10^{-1}	1.02	3.35×10^{-1}	1.01
5.21×10^{-2}	19704	6568	1.11×10^{-3}	5.45	7.73×10^{-2}	1.01	3.25×10^{-1}	1.
2.6×10^{-2}	80808	26936	1.2×10^{-4}	5.42	3.07×10^{-2}	1.01	3.21×10^{-1}	1.
1.3×10^{-2}	327036	109012	1.77×10^{-5}	5.23	1.18×10^{-2}	1.01	3.16×10^{-1}	1.

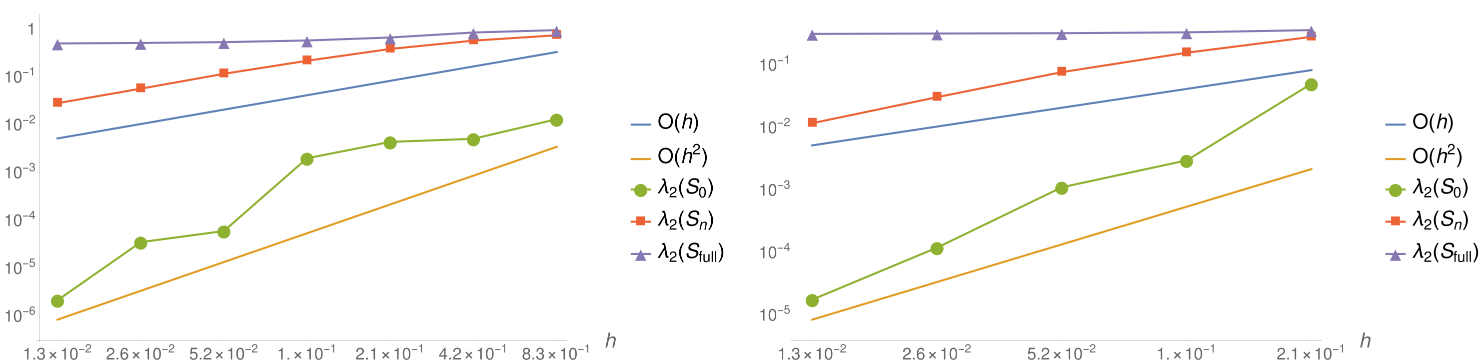

Figure 2: Log-log plot of λ_2 for Tables 1a (left) and 1b (right)

Table 2: Spectrum of (5) for $\mathbf{P}_2-P_1$

(a) $\Gamma = \Gamma_{\text{sph}}$

h	$n_{\mathbf{A}}$	$n_{\mathbf{S}}$	$\mathbf{S}_0$		$\mathbf{S}_n$		$\mathbf{S}_{\text{full}}$	
			λ_2	$\lambda_{n_{\mathbf{S}}}$	λ_2	$\lambda_{n_{\mathbf{S}}}$	λ_2	$\lambda_{n_{\mathbf{S}}}$
8.33×10^{-1}	789	51	3.22×10^{-1}	1.73	8.27×10^{-1}	1.17	9.68×10^{-1}	1.07
4.17×10^{-1}	3240	190	9.17×10^{-2}	1.08	6.45×10^{-1}	1.	8.56×10^{-1}	1.
2.08×10^{-1}	11718	664	1.78×10^{-1}	8.31×10^{-1}	5.49×10^{-1}	1.	6.75×10^{-1}	1.
1.04×10^{-1}	48762	2764	1.04×10^{-1}	8.35×10^{-1}	5.14×10^{-1}	1.	5.82×10^{-1}	1.
5.21×10^{-2}	193014	10912	2.99×10^{-3}	9.89×10^{-1}	5.02×10^{-1}	1.	5.34×10^{-1}	1.
2.6×10^{-2}	775998	43864	1.17×10^{-3}	7.9×10^{-1}	4.96×10^{-1}	1.	5.17×10^{-1}	1.

(b) $\Gamma = \Gamma_{\text{tor}}$

h	$n_{\mathbf{A}}$	$n_{\mathbf{S}}$	$\mathbf{S}_0$		$\mathbf{S}_n$		$\mathbf{S}_{\text{full}}$	
			λ_2	$\lambda_{n_{\mathbf{S}}}$	λ_2	$\lambda_{n_{\mathbf{S}}}$	λ_2	$\lambda_{n_{\mathbf{S}}}$
2.08×10^{-1}	5184	324	9.92×10^{-2}	3.89	1.33×10^{-1}	1.37	1.75×10^{-1}	1.19
1.04×10^{-1}	27906	1580	1.46×10^{-2}	4.35	2.84×10^{-1}	1.04	2.99×10^{-1}	1.02
5.21×10^{-2}	116568	6568	6.08×10^{-3}	4.85	3.19×10^{-1}	1.01	3.24×10^{-1}	1.01
2.6×10^{-2}	477660	26936	1.36×10^{-3}	4.92	3.14×10^{-1}	1.01	3.16×10^{-1}	1.

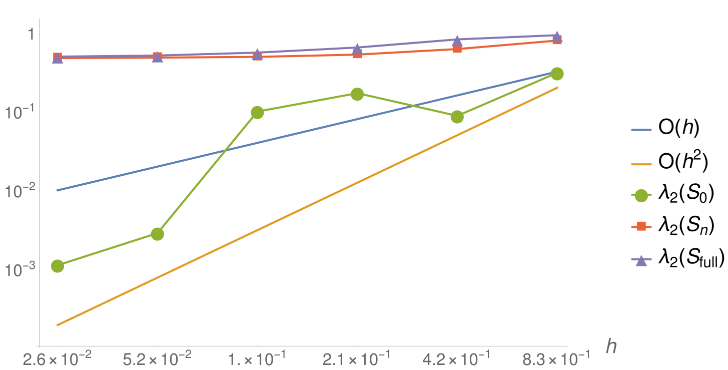

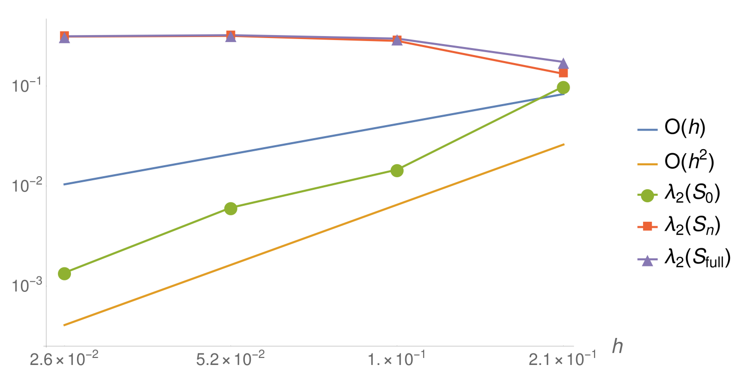

Figure 3: Log-log plot of λ_2 for Tables 2a (left) and 2b (right)

4 Numerical results: sensitivity of the spectrum to levelset shifts

In this section we investigate the sensitivity of the spectrum to levelset shifts

$$\Gamma \mapsto \Gamma + \alpha\, \mathbf{s}, \tag{8}$$

for some $\alpha \in \mathbb{R}$ and $\mathbf{s} \in \mathbb{R}^3$, $\|\mathbf{s}\| = 1$.

We construct the bulk mesh Ω_h^Γ and then perform the assembly of matrices (1) using the shifted levelset (8). That is, the refinement of Ω_h^Γ is performed using Γ, not $\Gamma + \alpha\, \mathbf{s}$, and $\Omega_h^{\Gamma+\alpha\,\mathbf{s}}$ is never constructed. We choose $\alpha \in [0, h]$ to guarantee the appearance of "small cuts" in Ω_h^Γ.

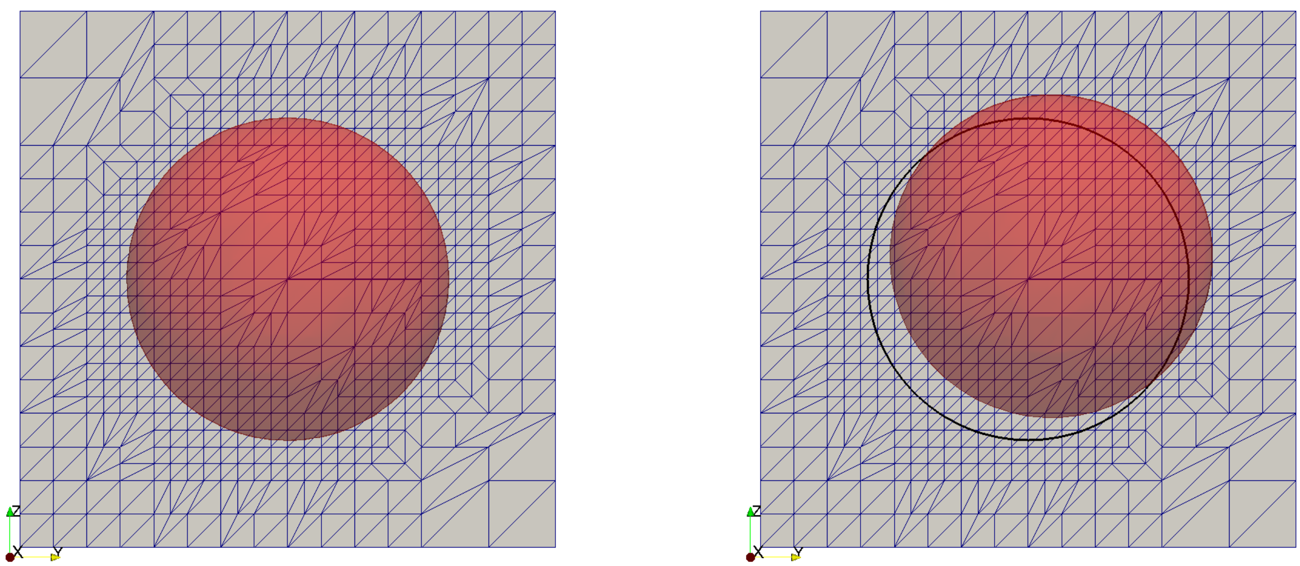

(a) Γ_{sph} (b) $\Gamma_{\mathrm{sph}} + \alpha\, \mathbf{s}$

Figure 4: The unit sphere (left) and the shifted unit sphere (right). Here $\mathbf{s} = (0, 1, 1)^T/\sqrt{2}$, $\alpha = 0.2$, and $h = 2.08 \times 10^{-1}$. The bulk mesh Ω_Γ^h is computed for Γ_{sph} and then used for $\Gamma_{\mathrm{sph}} + \alpha\, \mathbf{s}$

Table 3: Spectrum of (5) for perturbed levelset $\Gamma_{\text{sph}} + \alpha\,\mathbf{s}$. Here $\mathbf{s} = (1,1,1)^T/\sqrt{3}$, $h = 1.04 \times 10^{-1}$

(a) $\mathbf{P}_1 - P_1$

Surface	$\mathbf{S}_0$		$\mathbf{S}_n$		$\mathbf{S}_{\text{full}}$	
	λ_2	$\lambda_{n\mathbf{s}}$	λ_2	$\lambda_{n\mathbf{s}}$	λ_2	$\lambda_{n\mathbf{s}}$
Γ_{sph}	2.006×10^{-3}	7.79×10^{-1}	2.19×10^{-1}	1.	5.818×10^{-1}	1.
$\Gamma_{\text{sph}} + 0.1\,h\,\mathbf{s}$	4.832×10^{-4}	8.01×10^{-1}	2.195×10^{-1}	1.	5.818×10^{-1}	1.
$\Gamma_{\text{sph}} + 0.3\,h\,\mathbf{s}$	7.278×10^{-4}	8.17×10^{-1}	2.203×10^{-1}	1.	5.818×10^{-1}	1.
$\Gamma_{\text{sph}} + 0.5\,h\,\mathbf{s}$	3.121×10^{-4}	8.67×10^{-1}	2.221×10^{-1}	1.	5.82×10^{-1}	1.
$\Gamma_{\text{sph}} + 0.7\,h\,\mathbf{s}$	1.438×10^{-3}	1.51	2.254×10^{-1}	1.	5.82×10^{-1}	1.
$\Gamma_{\text{sph}} + h\,\mathbf{s}$	1.79×10^{-3}	2.07	2.332×10^{-1}	1.	5.827×10^{-1}	1.

(b) $\mathbf{P}_2 - P_1$

Surface	$\mathbf{S}_0$		$\mathbf{S}_n$		$\mathbf{S}_{\text{full}}$	
	λ_2	$\lambda_{n\mathbf{s}}$	λ_2	$\lambda_{n\mathbf{s}}$	λ_2	$\lambda_{n\mathbf{s}}$
Γ_{sph}	1.041×10^{-1}	8.35×10^{-1}	5.138×10^{-1}	1.	5.841×10^{-1}	1.
$\Gamma_{\text{sph}} + 0.1\,h\,\mathbf{s}$	1.705×10^{-3}	8.58×10^{-1}	5.138×10^{-1}	1.	5.841×10^{-1}	1.
$\Gamma_{\text{sph}} + 0.3\,h\,\mathbf{s}$	2.293×10^{-3}	8.81×10^{-1}	5.137×10^{-1}	1.	5.841×10^{-1}	1.
$\Gamma_{\text{sph}} + 0.5\,h\,\mathbf{s}$	5.63×10^{-3}	9.35×10^{-1}	5.138×10^{-1}	1.	5.844×10^{-1}	1.
$\Gamma_{\text{sph}} + 0.7\,h\,\mathbf{s}$	8.188×10^{-3}	1.77	5.138×10^{-1}	1.	5.843×10^{-1}	1.
$\Gamma_{\text{sph}} + h\,\mathbf{s}$	1.93×10^{-2}	2.21	5.142×10^{-1}	1.	5.852×10^{-1}	1.

References

[1] M. Olshanskii, A. Quaini, A. Reusken, and V. Yushutin. A finite element method for the surface stokes problem. *SIAM Journal on Scientific Computing*, 40(4):A2492–A2518, 2018.